arXiv:math/0001075v1 [math.NA] 13 Jan 2000

NUMERICAL INVESTIGATION OF A DIPOLE TYPE SOLUTION FOR UNSTEADY GROUNDWATER FLOW WITH CAPILLARY RETENTION AND FORCED DRAINAGE

EUGENE A. INGERMAN and HELEN SHVETS
Department of Mathematics,
University of California, Berkeley and
Lawrence Berkeley Laboratory, CA 94720
eugening@math.berkeley.edu, shvets@math.berkeley.edu

Abstract. A model of unsteady filtration (seepage) in a porous medium with capillary retention is considered. It leads to a free boundary problem for a generalized porous medium equation where the location of the boundary of the water mound is determined as part of the solution. The numerical solution of the free boundary problem is shown to possess self-similar intermediate asymptotics. On the other hand, the asymptotic solution can be obtained from a non-linear boundary value problem. Numerical solution of the resulting eigenvalue problem agrees with the solution of the partial differential equation for intermediate times. In the second part of the work, we consider the problem of control of the water mound extension by a forced drainage.

1. Introduction.

In the present work two problems from the theory of filtration through a horizontal porous stratum are considered. First we study a short, but intense, flooding followed by natural outflow through the vertical face of an aquifer. Further, we consider the possibility to control the spreading of the water mound by use of forced drainage at the boundary.

An important practical example of such a problem is groundwater mound formation and extension following a flood, after a breakthrough of a dam, when water (possibly contaminated) enters and then slowly extends into a river bank.

Consider an aquifer that consists of a long porous stratum with an impermeable bed at the bottom and a permeable vertical face on one side (Fig. 1). The space coordinate x is directed along the horizontal axis with $x = 0$ at the vertical face. A water reservoir is located in

Date: February 1, 2008.

the region $x < 0$. We assume that the flow is homogeneous in the y-direction. The height of the resulting mound is denoted by $z = h(x,t)$. The initial level of water in the stratum is assumed to be negligible.

The problem is formulated as follows. At some time $t = -\tau < 0$, the water level at the wall begins to rise rapidly, and water enters the porous medium. By time $t = 0$, the water level at the vertical face returns to the initial one.We assume that the distribution at time $t = 0$ is given by $h(x,0) = h_0(x)$ and is concentrated over a finite region $[0,d]$ (compactly supported). We also assume that $h_0(x)$ is concave down and $h_0^2(x)$ is gently sloping.

In problem 1, water naturally seeps through the boundary back into the reservoir, giving the boundary condition $h(0,t) = 0$. Inclusion of the effects of capillary retention into the model distinguishes our case from the well know dipole-type problem. The numerical and asymptotic solutions for the source-type boundary conditions were obtained in [6]. Most recently, the dipole-type problem with capillary retention was studied numericaly and analytically, using Lie-group techniques, by B. Wagner in [7].

Analysis and numeric computations show that in the case of natural outflow, the water mound is not extinguished in finite time. The outflow rate cannot be further increased by lowering the level at the boundary. In problem 2, in order to control the spreading of the water mound, forced drainage is introduced. The problem formulation was proposed in [3], where a complete mathematical derivation and rigorous analysis can be found. The forced drainage can be implemented, for instance, by drilling a number of holes or horizontal wells near the impermeable bottom. In this way, an additional discharge rate is created, and the fluid level becomes zero on some interval $[0, x_l(t)]$.

These are certainly highly idealized problems, but their solutions allow one to extract the qualitative properties and to check the numerical methods in solving more realistic problems.

2. Porous medium equation with capillary retention.

In the case of seepage and gently sloping profile $h^2(x,t)$ and in the absence of capillary retention, the model of flow in a porous stratum is described by the Boussinesq equation ([4] see also [2],[1]):

$$\partial_t h = \kappa \partial_{xx} h^2. \tag{2.1}$$

Here $\kappa = k\rho g/2\mu m$, k is the permeability of the medium, m its porosity (the fraction of the volume in the stratum which is occupied by the pores), ρ the fluid density, μ its dynamic viscosity, and g the acceleration of gravity. According to the hydrostatic law, water pressure

$p = \rho g(h - z)$. Then, the total head $H = p + \rho g z = \rho g h$ is constant throughout the height of the mound. Under the assumption of seepage and gently sloping profiles h^2, Darcy law is used to obtain the relation for the total flux $q = -\frac{k}{\mu}\nabla H \cdot h$.

Mathematical properties of the Boussinesq equation are well known [5]. An essential feature of this equation is the finite speed of disturbance propagation given a finite (compactly supported) initial distribution. Another important feature of this equation is the existence of special self-similar solutions. The graphs of such a solution for any two times t_0 and t_1 are related via a similarity transformation [1]. The special solutions, themselves corresponding to certain, sometimes artificial, initial and boundary conditions, are important because they provide intermediate asymptotics for a wide class of initial value problems. For these problems, the details of the initial distribution affect the solution only in the beginning; after some time, the solution approaches a self-similar asymptotics. The Boussinesq equation has been studied extensively and a number of self-similar solutions, for different boundary conditions, have been constructed ([2], [3]).

Following [1], [6], the Boussinesq equation can be modified to incorporate the effects of capillary retention into the model. If we exclude the possibility of water reentering the region that was filled with water at some earlier time and assume that initially the stratum is empty, we have the following situation: when water enters a pore, it occupies the entire volume, allowed by active porosity; when water leaves the pore, a fraction δ of the pore volume remains occupied by the trapped water. We assume that δ is constant. Let us denote the initial active porosity by m. Then, when water is entering previously unfilled pores, the effective porosity is m; when water is leaving previously water-filled pores, the effective porosity becomes $m(1 - \delta)$. Hence, in the presence of capillary retention, porosity depends on the sign of $\partial_t h(x, t)$. Notice, that permeability can be assumed unaffected, as the effect of capillary forces on permeability is significant only for small and/or dead-end pores, whose contribution to the total flux, in the first approximation, can be neglected.

The rate of change in the amount of water ΔV inside a volume element (Fig. 1) is equal to:

$$\Delta V = \begin{cases} m\frac{\partial h}{\partial t}\Delta x & \text{if } \frac{\partial h}{\partial t} > 0\ , \\ m(1-\delta)\frac{\partial h}{\partial t}\Delta x & \text{if } \frac{\partial h}{\partial t} < 0. \end{cases} \tag{2.2}$$

On the other hand, the rate of change in the volume of water due to the flux through the faces of a volume element $(x, x + \Delta x)$ is equal to

$$\Delta x\, \partial_x(\frac{k}{\mu}\partial_x H \cdot h) = \Delta x\, \frac{k\rho g}{2\mu}\partial_{xx}(h^2). \tag{2.3}$$

We denote $\kappa_1 = \frac{k\rho g}{2\mu m}$ and $\kappa_2 = \frac{k\rho g}{2\mu m(1-\delta)}$. Then, using the continuity of flux (no sources inside the water mound) and the balance of mass we obtain:

$$\frac{\partial h}{\partial t} = \begin{cases} \kappa_1 \partial_{xx}(h^2) & \text{if } \frac{\partial h}{\partial t} > 0\ , \\ \kappa_2 \partial_{xx}(h^2) & \text{if } \frac{\partial h}{\partial t} < 0. \end{cases} \tag{2.4}$$

This is a nonlinear parabolic partial differential equation with discontinuous coefficients, also known as the generalized porous medium equation [2], [6].

Continuity of the flux $q = -\frac{\rho g k}{\mu} h \cdot \partial_x h$ implies that at the mound tip x_r, where mound height is zero, the flux is also zero. For problem 1, these considerations lead to the following initial and boundary conditions to supplement equation (2.4):

$$\begin{aligned} h(x,0) &= h_0(x) \geq 0 \text{ (where } h_0(x) = 0 \text{ for } x \geq d), \\ h(x,t) &= 0,\ \partial_x h^2(x,t) = 0 \text{ at } x = x_r, \\ h(0,t) &= 0. \end{aligned} \tag{2.5}$$

The second line in (2.5) corresponds to the free boundary conditions on the right boundary, $x_r(t)$, which is unknown a priori.

It should be noted that for the solution of equation (2.1) (but not for (2.4)) with boundary conditions (2.5) the dipole moment is constant:

$$Q = \int_0^\infty x h(x,t)\, dx = C. \tag{2.6}$$

We call equation (2.4) with boundary conditions (2.5) a dipole-type problem. A similar problem, for source type initial and boundary conditions was considered in [6], see also [1].

For problem 2, the boundary conditions are changed to include the forced drainage condition. The discharge rate $q_0(t)$, which is a quantity that should be specified, determines the boundary condition at the left

free boundary x_l.

$$
\begin{aligned}
h(x,0) &= h_0(x) \geq 0 \text{ (where } h_0(x) = 0 \text{ for } x \geq d), \\
h(x,t) &= 0,\ \partial_x h^2(x,t) = 0 \text{ at } x = x_r, \\
h(x,t) &= 0,\ \partial_x h^2(x,t) = \frac{q_0(t)}{m\kappa} \text{ at } x = x_l\ .
\end{aligned} \tag{2.7}
$$

The second and third lines in (2.7) define, respectively, the free boundary condition on the right boundary and the forced drainage condition on the left boundary. Equation (2.4) together with boundary conditions (2.7) define problem 2.

3. Dimensional analysis of problem 1.

The parameters in the problem are $h, x, t, \kappa_1, \kappa_2, d$ - the initial width of the water mound, and $Q = Q(0)$ - the initial dipole moment. We can take the dimensions as follows: $[h] = H$, $[x] = L$, $[t] = T$. Then from equation (2.4) we have $[\kappa] = \frac{L^2}{TH}$. For the remaining parameters $[d] = L$, $[Q] = H \cdot L^2$. The dimensions for h and x are set to be independent. This can be done because the differential equation (2.4) is invariant with respect to the following group of transformations:

$$
x' = \alpha x,\ t' = \frac{\alpha^2}{\gamma} t,\ h' = \gamma h. \tag{3.1}
$$

The invariance insures that we can scale the units of measurement for h, while keeping the units for x unchanged.

The following dimensionless quantities can be obtained from these parameters:

$$
\Pi_1 = \frac{x}{(Q\kappa_1 t)^{1/4}}, \Pi_2 = \frac{d}{(Q\kappa_1 t)^{1/4}}, \Pi_3 = \frac{\kappa_1}{\kappa_2}, \text{and } \Pi = h(\frac{\kappa_1 t}{Q})^{1/2}.
$$

It follows that $\Pi = F(\Pi_1, \Pi_2, \Pi_3)$.

Since for large times, $t \gg \frac{\Delta x^4}{Q\kappa_1}$, the parameter $\Pi_2 \ll 1$, it would seem natural to set $\Pi = f(\Pi_1, \Pi_3)$, as in the case of $\kappa_1 = \kappa_2$, and look for a solution of the form:

$$
h = (\frac{Q^2}{\kappa_1 t})^{1/2} f(z, \frac{k_1}{k_2}),\ \text{where } z = \frac{x}{(Q\kappa_1 t)^{1/4}}. \tag{3.2}
$$

However, this leads to a contradiction when we consider an ordinary differential equation obtained from (2.4):

$$
(2f + \frac{df}{dz} z) = \begin{cases} -4\frac{d(f^2)}{dz^2} & \text{if } 2f + \frac{df}{dz} z < 0, \\ -4\frac{\kappa_1}{\kappa_2}\frac{d(f^2)}{dz^2} & \text{if } 2f + \frac{df}{dz} z > 0. \end{cases} \tag{3.3}
$$

Multiplying both sides by z we obtain an equation in total differentials, which is readily solved:

$$fz^2 = \begin{cases} -4(z\frac{df^2}{dz} - f^2) + C_1 & \text{if } 2f + \frac{df}{dz}z < 0, \\ -4\frac{\kappa_1}{\kappa_2}(z\frac{df^2}{dz} - f^2) + C_2 & \text{if } 2f + \frac{df}{dz}z > 0. \end{cases} \tag{3.4}$$

Observe that near $z = z_r$, where the height of the mound vanishes, the first equation holds. At $z = z_r$, h vanishes along with the flux, which is proportional to $\frac{\partial h^2}{\partial x}$. From the first equation at z_r, we obtain that $C_1 = 0$. Similarly, evaluating the second expression at $z = 0$, where $h = 0$, we find that $C_2 = 0$. Next, evaluating the two expressions at z_1, we obtain:

$$(\frac{df^2}{dz}(z_1)z_1 - f^2(z_1))(1 - \frac{\kappa_1}{\kappa_2}) = 0, \tag{3.5}$$

and using $2f + \frac{df}{dz}z = 0$ we obtain $-5f^2(z_1)(1 - \frac{\kappa_1}{\kappa_2}) = 0$. For $\kappa_2 = \kappa_1$, the solution can be found [2] and thus the assumption of complete similarity in Π_2 is correct. However, in the case of $\kappa_2 \neq \kappa_1$, we have $f(z_1) = 0$. This is a contradiction, because the change in sign of $\frac{\partial h(x,t)}{\partial t}$ should occur inside the mound, where the height is positive. Hence, the assumption of complete similarity for $\kappa_2 \neq \kappa_1$ does not hold.

We next solve the problem numerically and study the asymptotic behavior of the solution.

4. Numerical solution of the partial differential equation and further analysis for problem 1.

In order to simplify the numerical solution for equation (2.4) with free boundary conditions (2.5), we use a change of variables: $\xi = \frac{x}{x_r}$. We set $H(\xi, t) = h(x_r\xi, t)$, and equation (2.4) is transformed:

$$\partial_t H = \begin{cases} \frac{1}{x_r^2}(\kappa_1\partial_{\xi\xi}H^2(\xi,t) + \kappa_1\xi\partial_\xi H(1,t)\partial_\xi H(\xi,t)) & \text{if } \partial_t H(\xi,t) > 0, \\ \frac{1}{x_r^2}(\kappa_2\partial_{\xi\xi}H^2(\xi,t) + \kappa_1\xi\partial_\xi H(1,t)\partial_\xi H(\xi,t)) & \text{if } \partial_t H(\xi,t) < 0; \end{cases} \tag{4.1}$$

with boundary conditions $H(0,t) = H(1,t) = 0$. This effectively fixes the right boundary at $\xi = 1$.

The location of the free boundary $x_r(t)$ can be obtained in the course of the numerical solution in the following way. We assume that the solution is nearly stationary near the tip x_r and $h(x,t) \approx H(x - vt)$. Here, v denotes the instantaneous speed of mound extension, which changes slowly as a function of t. Then $\partial_t h \approx -v\partial_x h$ near x_r.

Considering equation (2.4) near the boundary x_r of the mound, where h is small, we have:

$$\partial_t h = \kappa_1 \partial_{xx} h^2(x,t) = 2\kappa_1((\partial_x h(x,t))^2 + h\,\partial_{xx} h(x,t)) \approx 2\kappa_1(\partial_x h(x,t))^2$$

so that

$$v(t) = -2\kappa_1 \partial_x h(x_r,t),\ x_r(t) = \int_0^t v(t)\,dt + x_r(0). \tag{4.2}$$

We solve the new boundary value problem numerically by using a forward-in-time, centered-in-space finite-difference approximation, where u_i^n is an approximation to the solution of (4.1) at the grid point (x_i, t_n):

$$\begin{aligned}
\kappa_i^n &= \begin{cases} \kappa_1 & \text{if } [(u_{i-1}^{n-1})^2 - 2(u_i^{n-1})^2 + (u_{i+1}^{n-1})^2] > 0, \\ \kappa_2 & \text{if } [(u_{i-1}^{n-1})^2 - 2(u_i^{n-1})^2 + (u_{i+1}^{n-1})^2] < 0; \end{cases} \\
u_i^{n+1} &= u_i^n + \frac{\Delta t}{\Delta x^2}\{\kappa_i^n[(u_{i-1}^n)^2 - 2(u_i^n)^2 + (u_{i+1}^n)^2] \\
&- \kappa_1 \xi_i (u_i^n - u_{i-1}^n)(u_N^n - u_{N-1}^n)\}/(x_r^n)^2, \\
x_r^{n+1} &= x_r^n - 2\kappa_1 \frac{\Delta t}{\Delta x}\,\frac{u_N - u_{N-1}}{x_r^n}.
\end{aligned}$$

In the numerical computation we start with an initial distribution of the source type, localized near $x = 0$ (Fig.2). Before the left free boundary reaches the point $x = 0$, the solution is of the source type and we can compare our numerical results to those in [6]. After some time t the left free boundary reaches $x = 0$, where it is thereafter fixed (Fig. 2).

Now we consider the scaled solution:

$$\frac{H(\xi,t)}{\max_\xi\ H(\xi,t)} = f(\xi, \frac{\kappa_1}{\kappa_2}),\ \xi = \frac{x}{x_r}. \tag{4.3}$$

We can see in Figs. 6 and 7 that as time t increases the numerical solution approaches a self-similar regime, so that the graphs of the scaled solution for different times "collapse" into a single curve. Moreover, Figs. 3 and 4 show a power-law dependence on time for both $\max_\xi H$ and x_r in the self-similar regime.

In part 3, we have shown that a self-similar solution of the first kind does not exist for this problem. To explain what happened we return to the dimensional analysis and look now for a generalized self-similar solution.

We have determined that the variables in the problem are related as follows: $\Pi = F(\Pi_1, \Pi_2, \Pi_3)$, where

$$\Pi_1 = \frac{x}{(Q\kappa_1 t)^{1/4}}, \Pi_2 = \frac{d}{(Q\kappa_1 t)^{1/4}}, \Pi_3 = \frac{\kappa_1}{\kappa_2}, \text{and } \Pi = h(\frac{\kappa_1 t}{Q})^{1/2}.$$

Our numerical investigation shows that for large t, as $\Pi_2 \to 0$:

$$F(\Pi_1, \Pi_2, \Pi_3) = \Pi_2^{\gamma} f_2(\Pi_1 \Pi_2^{-\varepsilon}, \Pi_3), \tag{4.4}$$

where γ and ε are constants. In fact, this is the next simplest situation after complete self-similarity and it is referred to as self-similarity of the second kind in Π_2 (see [2]).

Indeed, from the analysis above:

$$\begin{aligned} \frac{\Pi_1}{\Pi_2^{\varepsilon}} &= x d^{-\varepsilon} (t\kappa_1 Q)^{\frac{\varepsilon-1}{4}}, \\ \Pi_2^{\gamma} &= \frac{d^{\gamma}}{(t\kappa_1 Q)^{\gamma/4}}, \\ h(x,t) &= A\, t^{-\alpha} f(\frac{x}{B t^{\,\beta}}, \frac{\kappa_1}{\kappa_2}), \\ x_r(t) &= B t^{\beta}, \end{aligned} \tag{4.5}$$

where

$$A = (\kappa_1 Q)^{-\gamma/4} d^{\gamma}, B = d^{\varepsilon} (\kappa_1 Q)^{\frac{\varepsilon-1}{4}}, \alpha = \frac{\gamma+2}{4}, \text{and } \beta = \frac{1-\varepsilon}{4}.$$

The parameters α and β depend on the ratio $\frac{\kappa_1}{\kappa_2}$. They cannot be determined on the basis of dimensional analysis alone and have to be computed as a part of the solution. We will see that there is, actually, only one unknown parameter involved, since the differential equation provides an additional relation between α and β.

5. Derivation and numerical solution of a nonlinear eigenvalue problem.

The numerical solution of partial differential equation showed that there is indeed an intermediate asymptotic solution of the form (4.5). Now, we can obtain such a self-similar solution by transforming the problem of solving partial differential equation (2.4) with boundary conditions (2.5) into a nonlinear eigenvalue problem.

We substitute (4.5) into (2.4) and normalizing f so that $\frac{A}{B^2} = 1$ we get:

$$\partial_t h = -t^{-(\alpha+1)}\, A(\alpha f + \beta f' \xi), \tag{5.1}$$

$$\partial_{xx} h^2 = \frac{A^2 t^{-2\alpha} (f^2(\xi))''}{B^2 t^{2\beta}}, \tag{5.2}$$

$$\alpha f(\xi) + \beta f'(\xi)\xi = -\kappa^* (f^2(\xi))'' t^{-\alpha-2\beta+1}, \tag{5.3}$$

where

$$\kappa^* = \begin{cases} \kappa_1 & \text{if } ((1-2\beta)f + \beta f'\xi) < 0, \\ \kappa_2 & \text{if } ((1-2\beta)f + \beta f'\xi) > 0. \end{cases}$$

Since equation (5.3) cannot depend on time explicitly, $-\alpha - 2\beta + 1 = 0$. Finally, we get an ordinary differential equation:

$$(f^2)'' = \begin{cases} -(\beta f'\xi + (1-2\beta)f) & \text{if } ((1-2\beta)f + \beta f'\xi) < 0, \\ -\frac{\kappa_2}{\kappa_1}(\beta f'\xi + (1-2\beta)f) & \text{if } ((1-2\beta)f + \beta f'\xi) > 0. \end{cases} \tag{5.4}$$

The boundaries $x_0 = 0$ and $x_r = Bt^\beta$, in the new space variable, correspond to $\xi = 0$ and $\xi = 1$. The boundary condition at $\xi = 0$ becomes:

$$f(0) = 0. \tag{5.5}$$

For the right boundary, $\xi = 1$, we have:

$$f(1) = 0 \text{ and } (f^2)'(1) = 0. \tag{5.6}$$

From 5.4 and 5.6 it follows that $2\kappa_1(f'(1))^2 + \beta\xi f'(1) = 0$ and the tip conditions become:

$$f(1) = 0 \text{ and } f'(1) = -\frac{\beta}{2\kappa_1}. \tag{5.7}$$

The second order ODE (5.4) with three boundary conditions (5.7 and 5.5) constitutes a non-linear eigenvalue problem, which we now have to solve numerically. For each value of $\frac{\kappa_1}{\kappa_2}$, we find a value of β such that the boundary conditions are satisfied.

We use a high order, Taylor-expansion-based method to start the integration at $\xi = 1$ followed by a 4th order Runge-Kutta method and an iterative procedue to arrive at the value for β such that the third condition $f(0) = 0$ is satisfied. For computational convenience, we transform the differential equation by changing variables: $g(\xi) = f^2(\xi)$, so that $g(\xi)$ does not have a singularity at $\xi = 0$. In this manner, we obtain the dependence of β on $\frac{\kappa_1}{\kappa_2}$ (Fig. 5).

6. Comparison of the results for problem 1.

In logarithmic coordinates, we obtain from (4.5):

$$\log(u(1/2,t)) = -\alpha\log(t) + \log(A\, f(1/2, \frac{\kappa_1}{\kappa_2})) \tag{6.1}$$

$$\log(x_r(t)) = \beta\log(t) + \log(B) \tag{6.2}$$

i.e., straight lines with slopes $-\alpha$ and β.

From plots in Figs. 3 and 4, we can observe that after some initial time t both graphs approach straight lines. We repeat the calculations for a range of values of $\frac{\kappa_1}{\kappa_2}$.

Comparison of the results of the numerical solution of the nonlinear eigenvalue problem with the results obtained from the numerical solution to the partial differential equation (Fig. 5), shows that the two agree with high precision.

Also, the exact solution for the case $\kappa_1 = \kappa_2$ gives the value $\beta = .25$, which coincides with the results of the numerical computations with good accuracy.

7. Numerical solution of the partial differential equation for problem 2.

Although problems 1 and 2 are similar, the numerical treatment of problem 2 is more complicated. Time evolution of the left boundary in problem 2 makes rescaling, which was used in the numerical solution of problem 1, infeasible. Instead, we solve equation (2.4) on a grid, taking into account that the left and right boundaries may not fall onto gridpoints. We determine new positions of the boundaries from the numerical solution at each timestep.

Equation (2.4) is discretized using a forward-in-time, centered-in-space finite-difference scheme:

$$
\begin{aligned}
\kappa_i^n &= \begin{cases} \kappa_1 & \text{if } [(u_{i-1}^{n-1})^2 - 2(u_i^{n-1})^2 + (u_{i+1}^{n-1})^2] > 0, \\ \kappa_2 & \text{if } [(u_{i-1}^{n-1})^2 - 2(u_i^{n-1})^2 + (u_{i+1}^{n-1})^2] < 0; \end{cases} \\
u_i^{n+1} &= u_i^n + \tfrac{\Delta t}{\Delta x^2}\{\kappa_i^n[(u_{i-1}^n)^2 - 2(u_i^n)^2 + (u_{i+1}^n)^2]\}, \\
u_l^{n+1} &= u_l^n + \tfrac{2\Delta t}{\Delta x + \Delta x_l}\kappa_2^n\{\tfrac{(u_{l+1}^n)^2 - (u_l^n)^2}{\Delta x} - q^n\}, \\
u_r^{n+1} &= u_r^n + \tfrac{2\Delta t}{\Delta x + \Delta x_r}\kappa_1^n\{\tfrac{(u_{r-1}^n)^2 - (u_r^n)^2}{\Delta x} - \tfrac{(u_r^n)^2}{\Delta x_r}\}.
\end{aligned} \tag{7.1}
$$

Here u_l and u_r are the nonzero values of u on the grid, adjacent to the left and right boundaries respectively, q is the drainage flux, Δx_l and Δx_r are distances from the left and right boundaries to the grid points. We treat the values u_l and u_r separately in order to incorporate the boundary conditions and improve precision.

The location of the left boundary is obtained from the values of u:

$$
x_l^{n+1} = x_l^n + \Delta x_l - \frac{(u_l^n)^2}{q}. \tag{7.2}
$$

The right boundary location is obtained by extrapolation from the values of u^{n+1}.

We check the numerical method for $\kappa_1 = \kappa_2$ by comparing the numerical solution with a known analytic solution. The exact self-similar solutions for the problems with forced drainage are given in [3]. We choose a value of $\beta \neq .25$ and then solve an ordinary differential equation (5.3) with the initial condition (5.7). For $\beta < .25$ the solution $f(\xi)$ of the ordinary differential equation intersects the x-axis at some point $\xi = \lambda > 0$ and at $\xi = 1$.

From the solution of the ordinary differential equation we obtain a self-similar solution:

$$h(x,t) = Bt^{-(1-2\beta)} f(\frac{x}{At^{\beta}}) \tag{7.3}$$

of the partial differential equation. The locations of the free boundaries are given by $x_r(t) = At^{\beta}$, $x_l(t) = \lambda At^{\beta}$, and the drainage flux is given by $q(t) = mBAt^{-2+3\beta}(f^2)'(\lambda)$ (see [3]). We use the self-similar solution at some time t_0 as an initial value for the numerical solver, set drainage flux on the left boundary to be $q(t)$, and compute the solutions until time t_1. As in the analysis in section 6, the graphs of $x_r(t)$, $x_l(t)$ should be straight lines in logarithmic coordinates, and the graphs of the scaled solution for different times t should collapse into one curve. That's what we observe in Figs. 9 and 10.

Now, we try to model the conditions of a flood followed by forced drainage, as described in the introduction. We begin by computing the solution to problem 1 until some time t_0, which corresponds to the flood followed by natural drainage through the boundary of the aquifer. After t_0, we set a constant drainage flux $q(t) = q_0$ at the left boundary. In particular, we set q_0 to equal twice the natural drainage flux at time t_0. As we see in Fig. 12, the water mound, that has appeared after the flood, is completely extinguished in finite time.

8. Conclusion.

1. The numerical simulations of two problems involving drainage and capillary retention of the fluid a in porous medium were presented. It was shown that the problem with dipole type initial and boundary conditions has a self-similar intermediate asymptotics in the case of a porous medium with capillary retention.
2. A problem of control of the water mound extension by forced drainage was considered. The possibility of extinguishing the propagating water mound by creating a forced drainage flux $q(t)$ at the left boundary was confirmed numerically. Using our results, it should be possible to derive a cost efficient drilling regime and to localize the mound and contain the contamination inside a prescribed region.

It would be interesting to extend the numerical investigation above to the case of a fissurized porous medium.

9. Acknowledgements.

The authors are grateful to Professor G.I. Barenblatt, without whose direction and advice this work would not have been possible. The authors use this occasion to thank Professor A. Chorin for many helpful discussions of this work and for his constant attention and encouragement.

This work was supported in part by the Computational Science Graduate Fellowship Program of the Office of Scientific Computing in the Department of Energy, NSF grant contract DMS-9732710, and the Office of Advanced Scientific Computing Research, Mathematical, Information, and Computational Sciences Division, Applied Mathematical Sciences Subprogram, of the U.S. Department of Energy, under Contract No. DE-AC03-76SF00098.

References

1. G.I. Barenblatt, *Scaling, self-similarity, and intermediate asymptotics*, first ed., Cambridge University Press, New York, 1996.
2. G.I. Barenblatt, V.M. Entov, and V.M. Ryzhik, *Theory of fluid flows through natural rocks*, first ed., Kluwer Academic Publishers, Dordrecht, 1990.
3. G.I. Barenblatt and J.L. Vasquez, *A new free boundary problem for unsteady flows in porous media*, Euro. Jnl of Applied Mathematics **9** (1998), 37–54.
4. C.W. Fetter, *Applied hydrogeology*, third ed., Macmillan College Publishing Company, New York, 1988.
5. A.S. Kalashnikov, *Some problems of qualitative theory of the nonlinear second-order parabolic equations*, Russian Math. Surveys (1987), no. 42, 169–222.
6. I.N. Kochina, N.N. Mikhailov, and M.V. Filinov, *Groundwater mound damping.*, Int. J. Engng Sci **21** (1983), no. 4, 413–421.
7. B.A. Wagner, *Perturbation techniques and similarity analysis for the evolution of interfaces in diffusion and surface tension driven problems*, Zentrum Mathematik, TU Munchen, 1999.

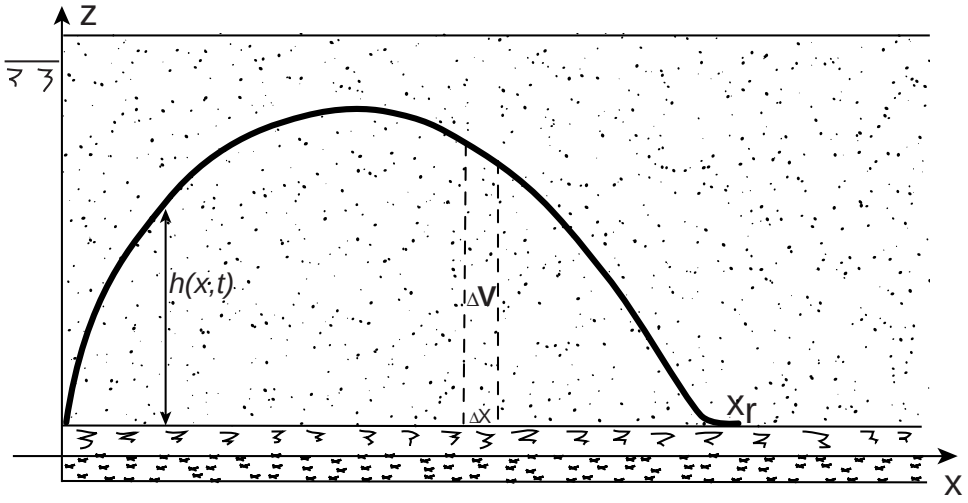

FIGURE 1. Groundwater dome extension in a porous medium.

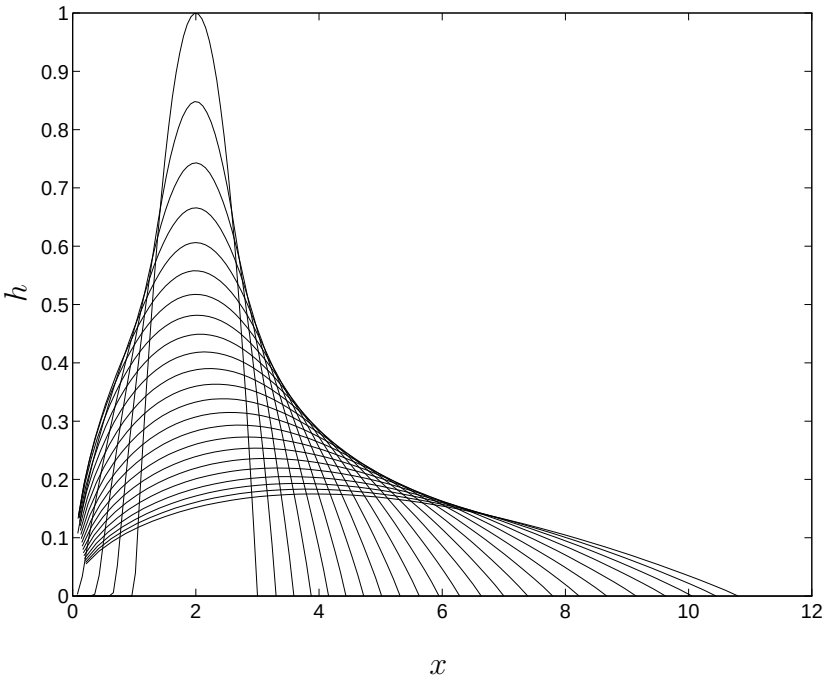

FIGURE 2. Evolution in time of the partial differential equation solution with $\frac{\kappa_1}{\kappa_2} = .5$ for time interval t=[0,18].

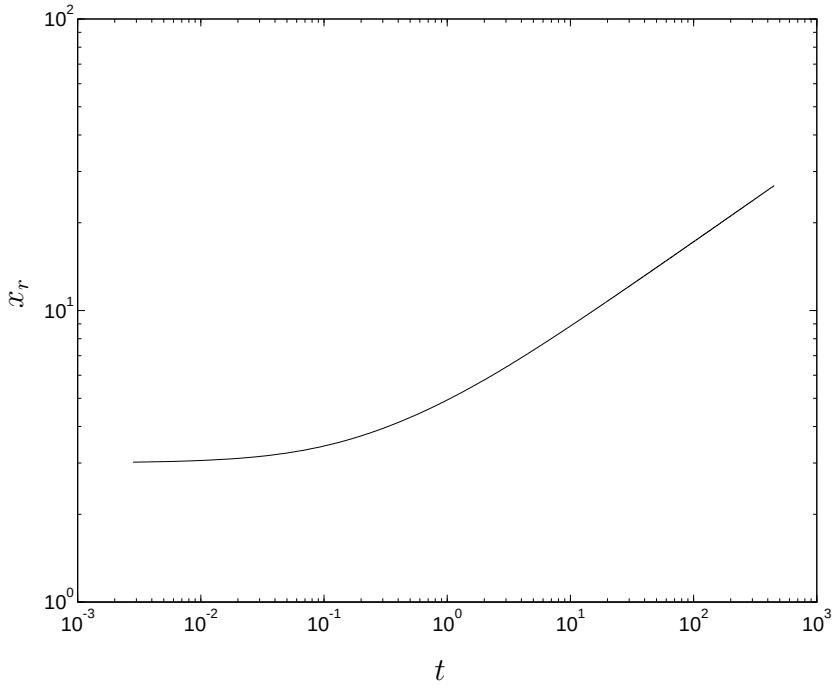

FIGURE 3. Example of the time evolution for the position x_r of the free boundary. Time interval $t = [0, 450]$. For this plot $\frac{\kappa_1}{\kappa_2} = .5$.

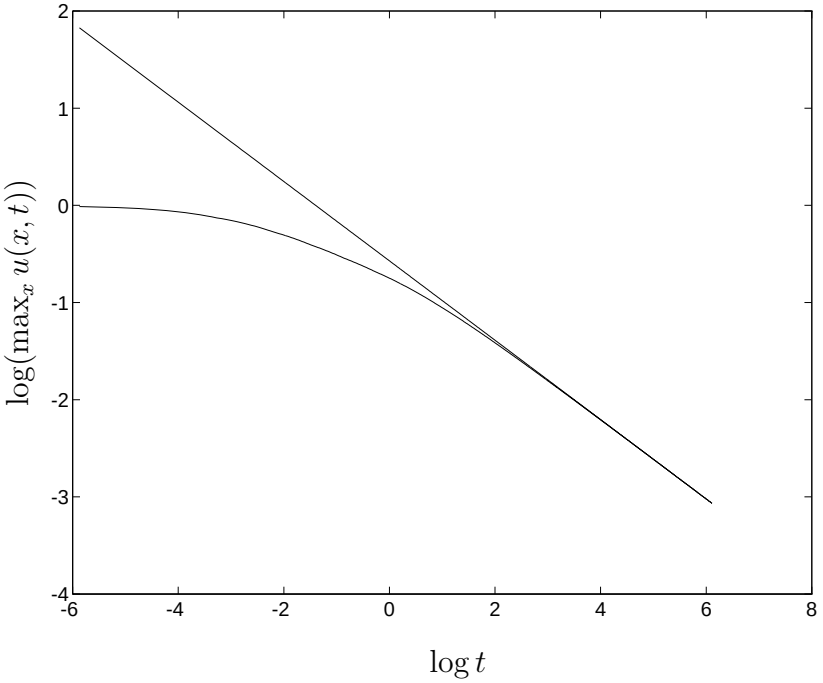

FIGURE 4. Plot of $\log(\max_x u(x,t))$ vs. $\log(t)$ with $\frac{\kappa_1}{\kappa_2} = .5$. The straight line shows a linear fit to the straight part of the graph.

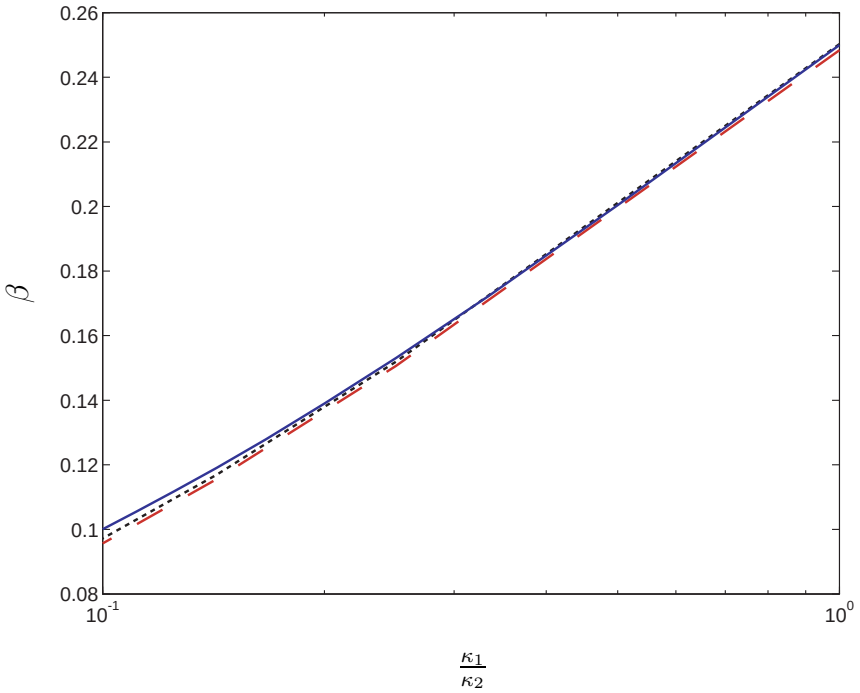

FIGURE 5. Plot of the dependence of β on $\frac{\kappa_1}{\kappa_2}$. The solid line is obtained from graph 4 for different values of $\frac{\kappa_1}{\kappa_2}$, by applying least-squares fit to the straight part of the graph and then using equation (6.1). The dashed line is obtained from graphs 3, by applying the procedure above and then (6.2). The dotted line is obtained from the solution of the nonlinear eigenvalue problem given by equation (5.4) with initial conditions 5.7 for different values of $\frac{\kappa_1}{\kappa_2}$.

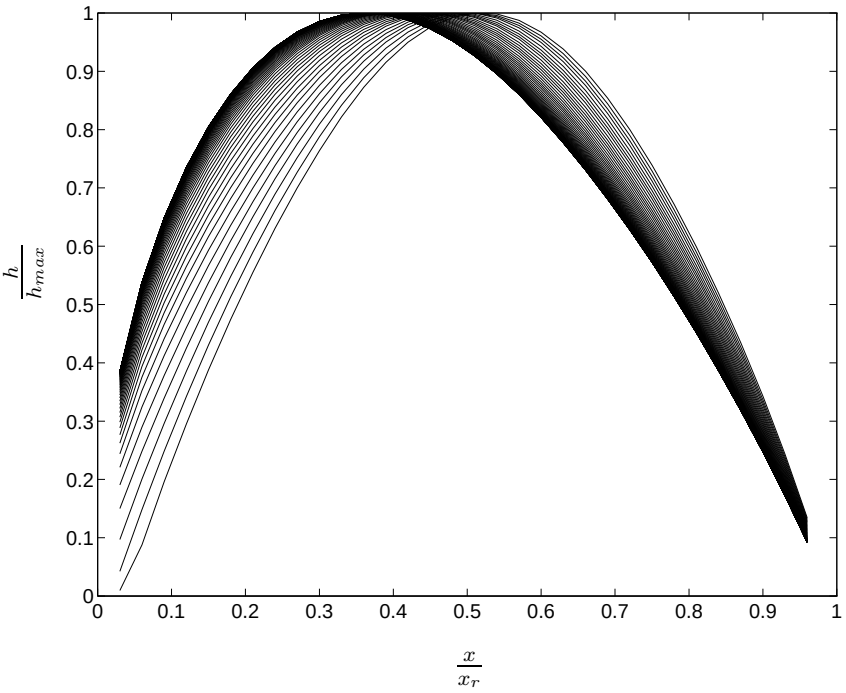

FIGURE 6. Plot of the scaled solution (4.3) of the partial differential equation for $t = [.2, 18]$. $(\frac{\kappa_1}{\kappa_2} = .5)$.

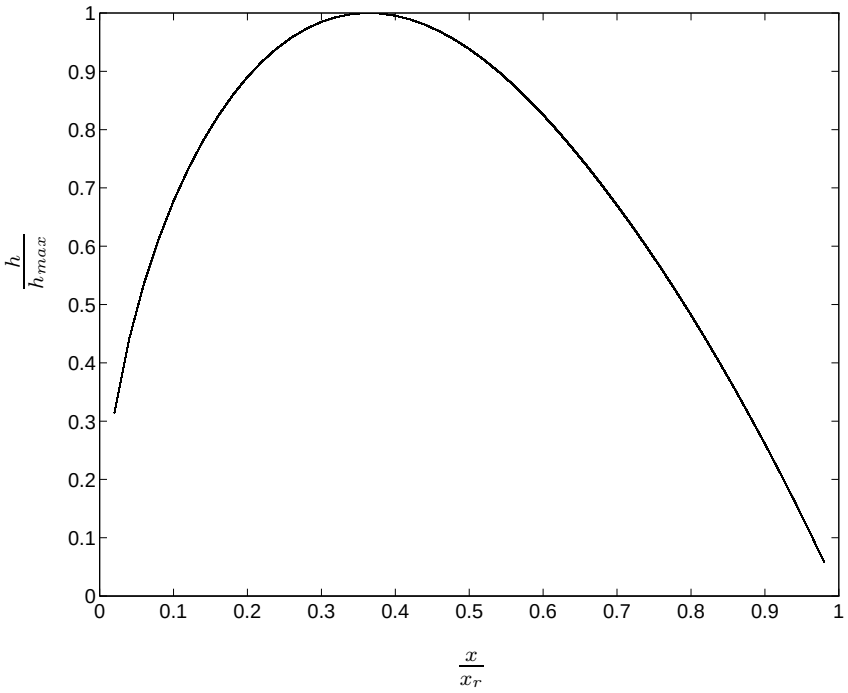

FIGURE 7. Plot of the scaled solution (4.3) of the partial differential equation for time interval $t = [18, 450]$. For this plot $\frac{\kappa_1}{\kappa_2} = .5$.

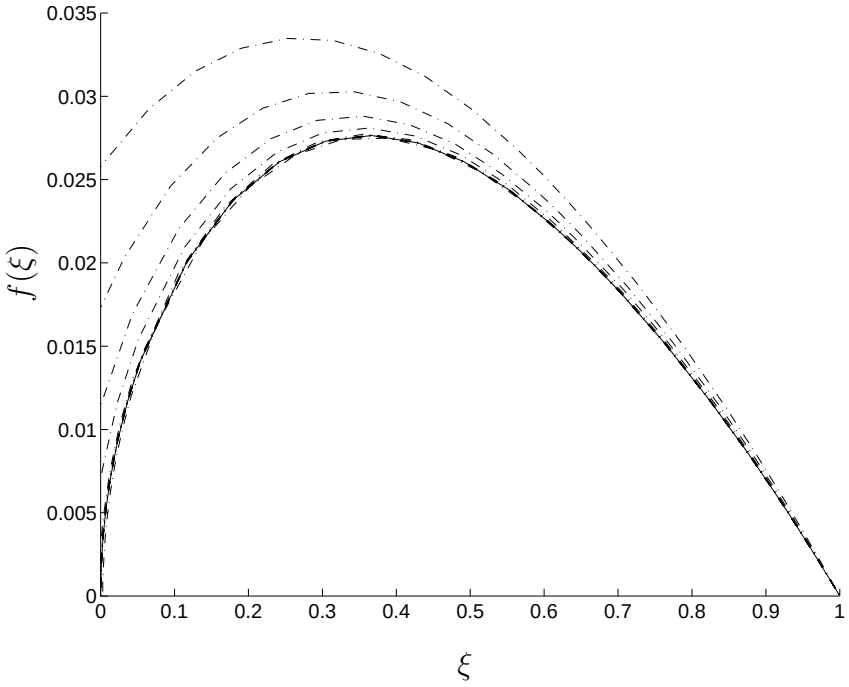

FIGURE 8. Example of convergence of the "shooting" method for solving the nonlinear eigenvalue problem given by (5.4), (5.7).

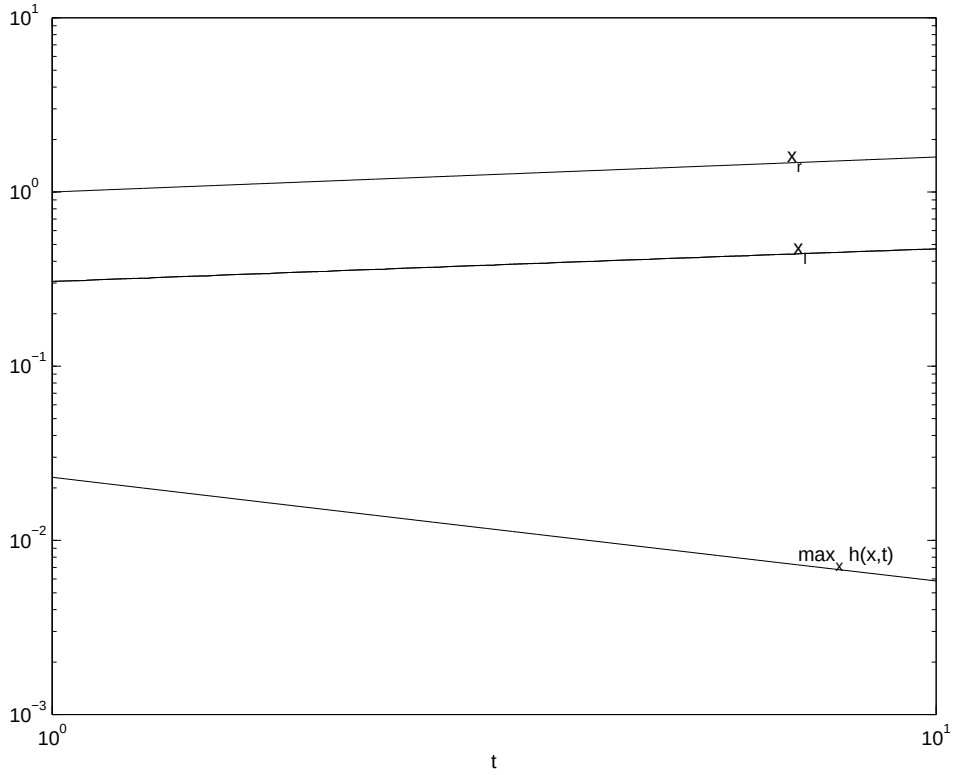

FIGURE 9. Positions of the boundaries and $\max_x h(x,t)$ vs t in logarithmic coordinates for the self-similar regime in the forced drainage problem. $\beta = .2$

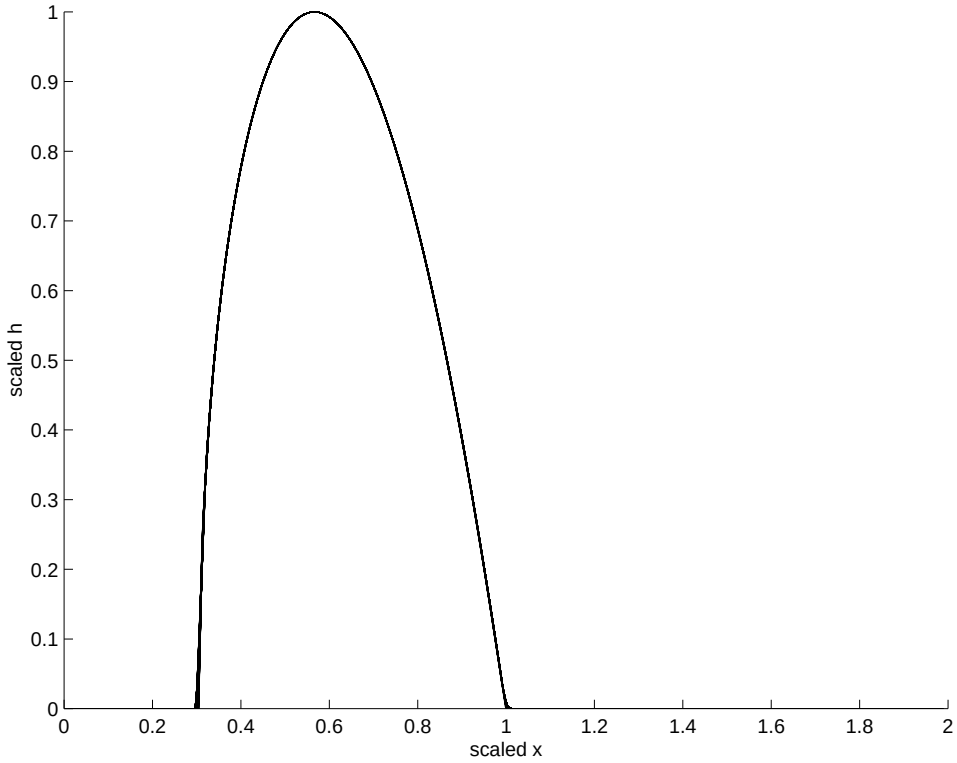

FIGURE 10. "Collapse" of the graphs of the scaled solution in self-similar coordinates for problem 2. Time $t = [1, 10]$, $\beta = .2$

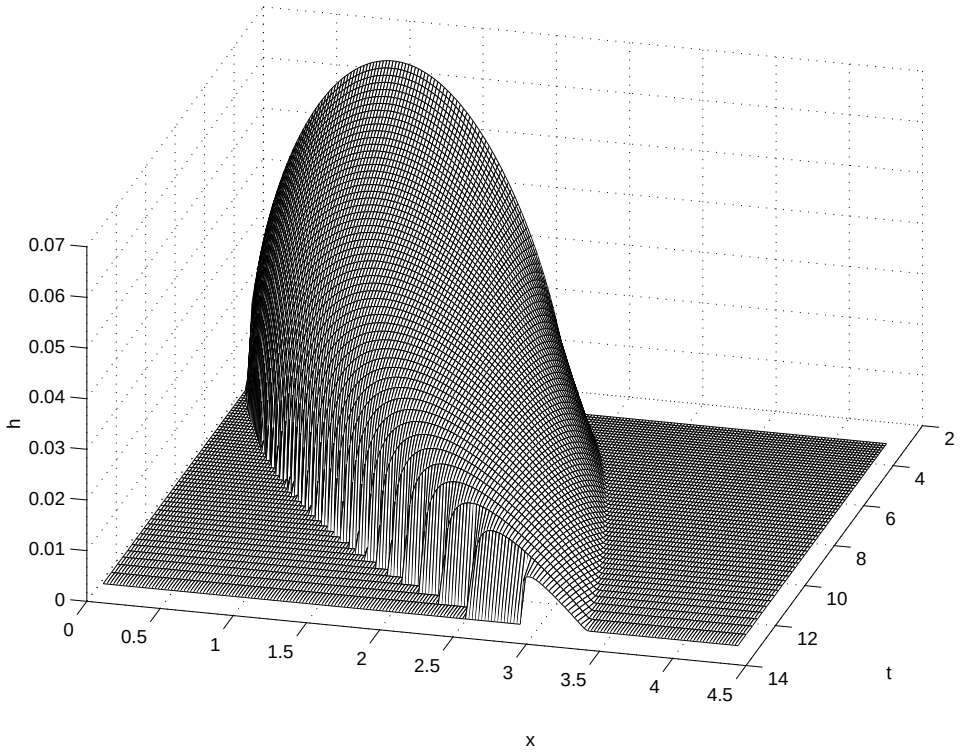

FIGURE 11. Evolution in time of the solution to the PDE with forced drainage.

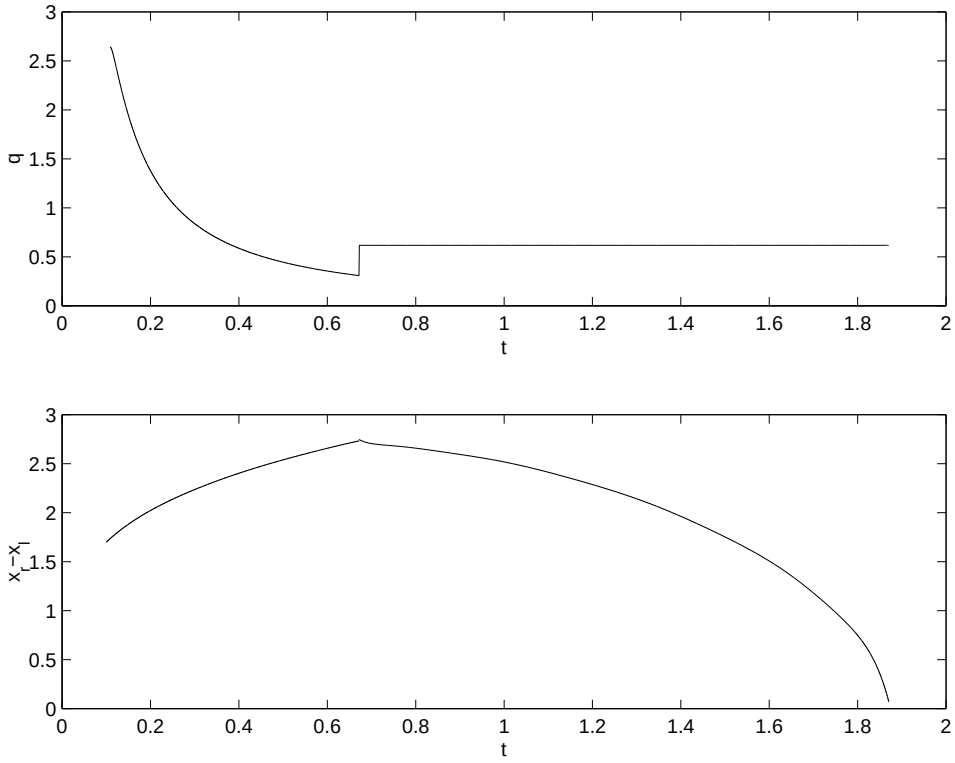

FIGURE 12. Extinguishing of the water mound with forced drainage.